F/A-18 Inlet/Engine Compatibility Flight Test Results

Nasim F. Amin*
Northrop Corporation, Hawthorne, California
and
David J. Hollweger*
McDonnell Douglas Corporation, St. Louis, Missouri

The U.S. Navy F/A-18A fighter aircraft inlet engine compatibility flight test results obtained during the full-scale development program are reviewed. All of the critical maneuvering conditions, both subsonic and supersonic, were flight tested with special emphasis on the aircraft prime combat maneuvering region. The instrumentation design and assessment approach used to successfully evaluate inlet/engine compatibility during the flight test program are also presented. The inlet rake, used to measure inlet distortion at the engine face, features 40 close-coupled low- and high-response probes, in an 8 leg, 5-ring configuration located 4 in. ahead of the engine nose dome. An analog distortion calculator is used to screen the large quantities of recorded high-response distortion data for subsequent digitization in selected regions of peak distortion. Dynamic distortion data and patterns are included that show increase in inlet distortion with angle of attack and sideslip. Dynamic inlet distortion has been measured on the instrumented aircraft at extreme maneuvering conditions. The distortion points fall within the engine distortion experience boundary. No engine stalls occurred during either the fixed- or variable-throttle compatibility testing for subsonic maneuvering excursions well beyond the design goal envelopes. Satisfactory engine operation has been demonstrated, and inlet distortion measured up to 65 deg angle of attack and 20 deg sideslip. Compatible subsonic maneuvering excursions well beyond the variable-throttle design goal envelopes are also demonstrated on the instrumented aircraft using the worst-case throttle transient (max-idle-max bodie). Inlet dynamic distortion levels during supersonic aircraft maneuvers are low and well within the engine distortion experience boundary.

Introduction

THE U.S. Navy's F/A-18A "Hornet" fighter aircraft built by McDonnell Douglas/Northrop is powered by two General Electric F404-GE-400 turbofan engines. The high maneuvering capability of the F/A-18A requires that its inlet/engine system be compatible at extreme angles of attack and side slip. Extreme aircraft maneuvers can cause high levels of dynamic inlet distortion at the engine face that exist for only a few milliseconds (i.e., time for one rotor revolution), but can adversely affect engine stability. Therefore, in order to assess inlet/engine compatibility, acquisition and analysis of high-response inlet data were required during the flight test program.

The rake design and location was mutually established by the aircraft and engine contractors to insure rake commonality between the inlet and engine development programs. Commonality is desirable since it eliminates several unknowns from the compatibility analysis.

The data acquisition and reduction system is similar to that used on the F-15 program.[1,2] An analog distortion calculator was used to edit the large quantities of recorded high-response distortion data for subsequent digitization in selected regions of peak distortion levels.

All of the compatibility flight testing was accomplished on the instrumented propulsion aircraft (F2). In order to show that the inlet/engine system is compatible throughout the aircraft maneuvering design goal envelopes, measured inlet distortion levels obtained during extreme aircraft maneuvers are compared with the engine distortion experience boundary established during the F404 engine development program. The comparison covers both fixed- and variable-engine throttles. All of the critical maneuvering conditions, both subsonic and supersonic, were flight tested with special emphasis on the F/A-18A prime combat maneuvering region.

The instrumentation design and assessment approach used to successfully evaluate inlet/engine compatibility during the full-scale development flight test program is presented. The effects of angle of attack and sideslip on inlet dynamic distortion are discussed. Dynamic distortion pressure patterns are also included to convey the range of dynamic distortion activity at the engine face during extreme aircraft maneuvering attitudes.

Air Induction System

The F/A-18 air induction system features single-ramp external compression inlets with a fixed geometry which are side-fuselage mounted and located approximately 25 ft aft of the aircraft nose under the leading-edge extension (LEX), as shown in Fig. 1. The inlets are separated from the fuselage by approximately 5 in. to avoid ingestion of the fuselage boundary layer. A blunt, cut-back lower cowl lip minimizes the inlet distortion at extreme subsonic maneuvering attitudes. During supersonic operation, compression is provided by LEX precompression and by a single oblique shock generated by the 5 deg compression ramp and a terminal normal shock. Controlled ramp boundary-layer bleed from the compression ramp minimizes shock/boundary-layer interaction at supersonic speeds.

Inlet Rake Design Criteria

Commonality between the flight test rake and the engine manufacturer's distortion test rake was established as a design requirement early in the F/A-18A program. The major impact of the commonality requirement was to change the inlet rake from an engine-mounted design adjacent to the engine face to an airframe-mounted design located 4 in. ahead of the engine nose dome. The engine face rake configuration was established using the commonality criteria in combination with the following detailed rake design criteria:

Presented as Paper 81-1393 at the AIAA/SAE/ASME Joint Propulsion Conference, Colorado Springs, Colo., July 27-29, 1981; submitted Aug. 7, 1981; revision received July 26, 1982.

*Senior Technical Specialist, F-18 Propulsion Analysis Department.

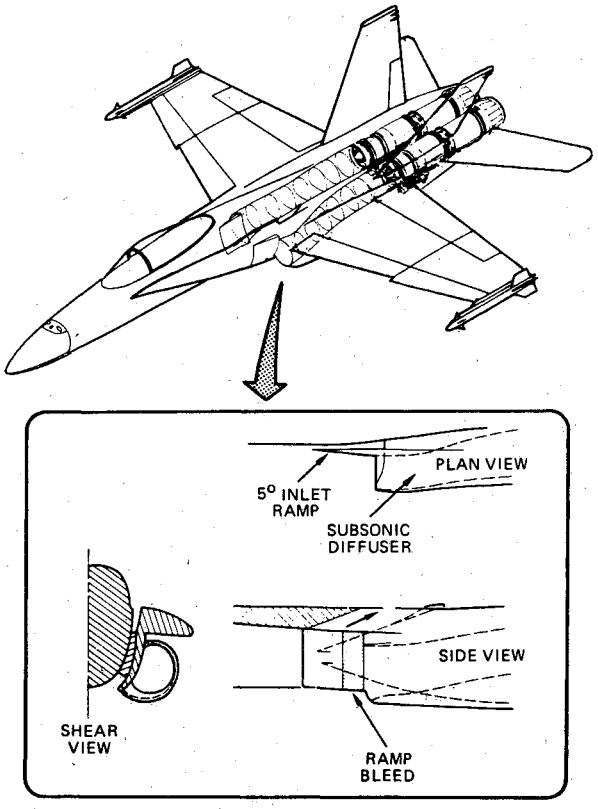

Fig. 1 F/A-18A air induction system.

Inlet/engine interface

1) Aerodynamic interface plane: the pressure measurement plane is 4.0 in. forward of the engine nose dome leading edge.

2) Number and position of measurements: 40 dual probes located at centers of equal area on 8 equally spaced rake legs with 5 probes per leg.

3) Dual-probe configuration; both low- and high-response probes are provided at each measurement position, using a geometrical configuration identical to the dual-probe configuration used for the F-15 inlet rake design.

4) Mounting position (airframe or engine): the inlet rake is airframe mounted.

5) Inlet flow blockage: minimum blockage consistent with structural and vibration limitations (about 8%).

Structure and vibration

1) Hammershock overpressure: rake legs are stressed to withstand a potential engine surge-induced hammershock.

2) Vibration: rake leg vibration characteristics are tuned such that the rake resonant frequencies fall outside the engine rotor 1/rev frequencies; N_1 range = 100-230 Hz, N_2 range = 190-280 Hz.

Installation considerations

1) Leakage: number of pneumatic connections is held to an absolute minimum in order to minimize the possibility of leakage.

2) High-response transducer replacement: all are replaceable with the inlet rake and the engine installed.

3) Low-response transducer replacement: all are replaceable with the rake installed in the aircraft but with the engine removed.

Sensor range and environment

1) Pressure range: 2-32 psia.

2) Temperature range: 65-250°F.

3) Frequency response: 0-1000 Hz.

4) Hammershock: transducers must survive exposure to potential engine surge-induced hammershock.

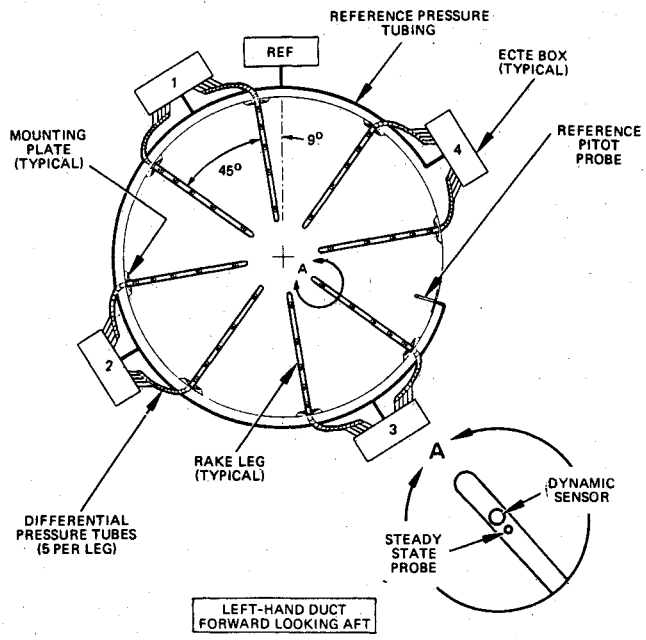

Fig. 2 F/A-18A engine face pressure measurement.

5) System accuracy as a percent of reading (2σ): at 2 psia 3.2%, at 5 psia 1.3%, and at 32 psia 1.0%.

Data acquisition system

1) Low-response data: 10 samples/s. using existing aircraft pulse code modulation (PCM) system.

2) High-response data: record continuously with accurate time correlation using existing aircraft narrow-band frequency modulation equipment.

Inlet Rake Instrumentation and Data Acquisition

The inlet rake used to measure inlet distortion at the engine face features 40 close-coupled low- and high-response probes in an 8-leg, 5-ring configuration, as shown in Fig. 2. Rake legs are equally spaced but clocked 9 deg from top dead center in order to minimize the aircraft installation impact. Each rake leg has five dual-probe pressure pickups and is attached to the duct wall using four fasteners through a mounting plate. The rake leg leading edges have an airfoil fairing that can be removed for access to the high-response transducers. Near the inlet diffuser wall, each rake leg trailing edge is extended back to the engine face to provide a tube and wire route into the engine bay.

The plane of instrumentation is located in a region of approximately constant duct area 4.0 in. forward of the engine nose dome leading edge, as shown in Fig. 3. Both low- and high-response probes are provided at each of the 40 instrumentation locations. The low-response probes are located at the centroid of five equal, annular areas. Each high-response probe is located 0.304 in. away from its corresponding low-response probe. The plane of instrumentation is located 4.8 chord thicknesses upstream of the maximum cross section of the strut to minimize the effects of the strut on the measured data.

The dual low- and high-response probe configuration was developed for the F-15 inlet rake in order to satisfy frequency and accuracy requirements over the aircraft pressure and temperature operating ranges. Flat frequency response to 1000 Hz requires that the high-response transducers be mounted on the inlet rake legs. The temperature extremes to which the rake legs are exposed can induce significant errors in the high-response transducer signals. The greater portion of this error is transducer zero shift with temperature. High-pass filters eliminate the zero-shift error from the high-response data. Therefore, the high-response transducers are designed

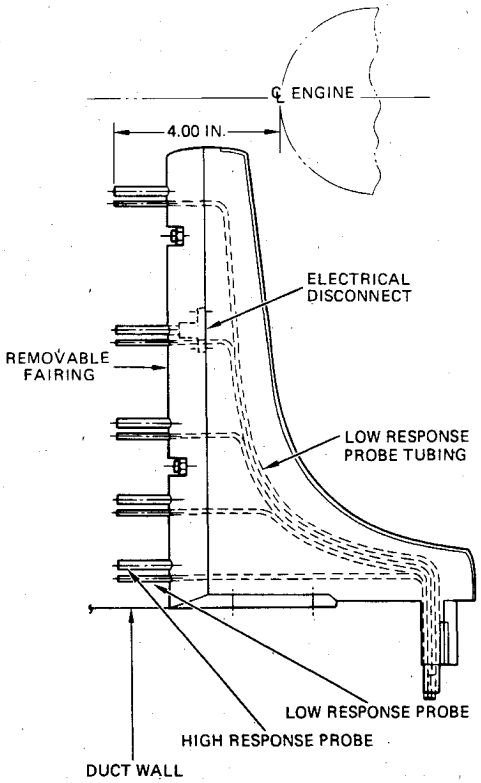

Fig. 3 Typical rake leg.

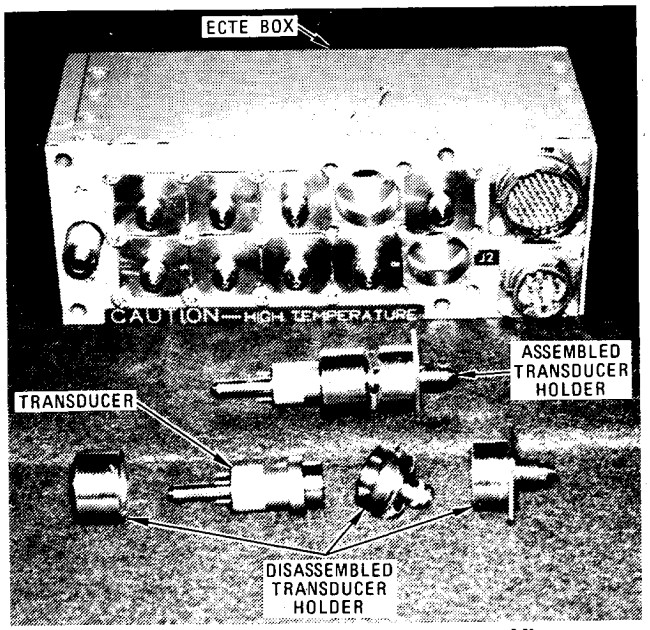

Fig. 4 ECTE box and transducer holder assemblies.

for minimum variation in sensitivity throughout the temperature range. The low-response transducers are placed in temperature-controlled enclosures to minimize temperature-induced errors in the steady-state data.

Low-Frequency Response Pressure Measurement System

The low-response (0-0.25 Hz) pressures are measured using the differential pressure measurement system shown schematically in Fig. 2. A differential measurement system was selected so that one set of transducers could be used to cover the entire aircraft pressure range and still meet the accuracy requirements of the detailed design criteria. The 40 low-response pressures are measured using 40 differential pressure transducers mounted in groups of 10 within 4 environmentally controlled transducer enclosures (ECTE boxes). The system reference pressure is supplied by a separate duct wall-mounted pitot probe, which is measured by two absolute pressure transducers mounted in a fifth ECTE box. The reference pitot probe is connected to the reference side of the four differential transducer ECTE boxes and to the reference transducer ECTE box using 0.25 in. o.d tubing.

The low-response differential pressure at each measurement position on the rake is sensed through 30 in. of 0.125 in. o.d. tubing. Each tube is routed through its associated rake leg into the engine bay (Fig. 3). The steady-state pressure tubes from each adjacent pair of rake legs are routed to 10 differential pressure transducers mounted in an ECTE box.

The Statham PM 856-15 differential transducer selected for this application is a thin-film, flush diaphragm, strain gage transducer. The transducer range (±15 psia) was selected so that the transducer could withstand a potential engine stall-induced hammershock without breaking the transducer diaphragm. For normal measurement, the transducers were spanned from −1 to +5 psia or less.

Primary considerations in the selection of the low-response reference pressure transducer were size, accuracy, reliability, and temperature characteristics. The Statham PA 822-40-301 absolute transducer was selected for this application with a range of 0-40 psia to satisfy the design criteria.

ECTE Box Design

The environmentally controlled transducer enclosures (ECTE boxes) are designed to accommodate 10 differential pressure transducers. The transducers are placed in individual three-piece transducer holders and inserted and fastened into the ECTE box transducer mounting block, as shown in Fig. 4. Any one transducer can be removed and replaced without disturbing the other nine. Three high-temperature O-ring seals are used to establish this quick-disconnect pneumatic seal, one on the reference pressure side and two on the differential pressure side. The reference side pressure is supplied to the individual transducers through passages machined into the transducer mounting block.

ECTE box temperature is established by thermostatically controlled electrical heater rods embedded in the transducer mounting block. The aluminum mounting block conducts the heat uniformly around all of the transducers. Because both rapid warmup and accurate temperature control are required, the heater system has two circuits. An ac powered, thermostatically controlled 77 W heater circuit provides additional power during warmup. A dc powered, proportionally controlled 86 W heater circuit holds the temperature at 225 ± 5°F. Each ECTE box has two electrical connectors, one to accommodate the excitation and signal wiring for the 10 transducers and one to accommodate the heater element wiring for temperature control.

The above description applies to the four ECTE boxes that accommodate the 40 differential low-response transducers. The same design was used for the fifth ECTE box, except for a modification to accommodate the two larger absolute-pressure reference transducers.

Transducer Tubing

The location of the low-response differential transducers in the ECTE boxes mounted on the engine face bulkhead provides easy access to the transducers after engine removal and permits use of short (30 in.) tubes from the probes to the transducers. Analysis indicates that these short lengths of 0.125 in. o.d. tubing insure satisfactory amplitude and phase response in the low-frequency range (Fig. 5). It is this need for short lengths of tubing that established the ECTE box requirement for the low-response differential transducers.

Tubing is also routed from the reference pitot probe to the five ECTE boxes. Larger tubing (0.25 in. o.d.) is used to

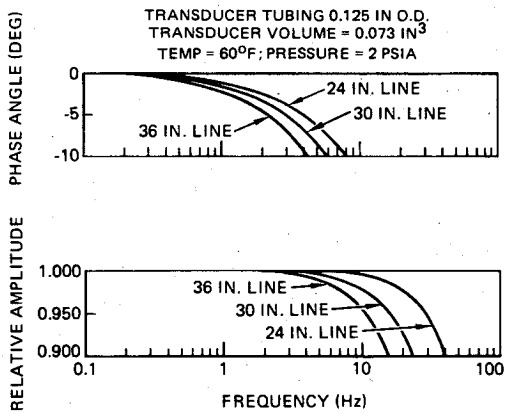

Fig. 5 Frequency response of pressure transmission line.

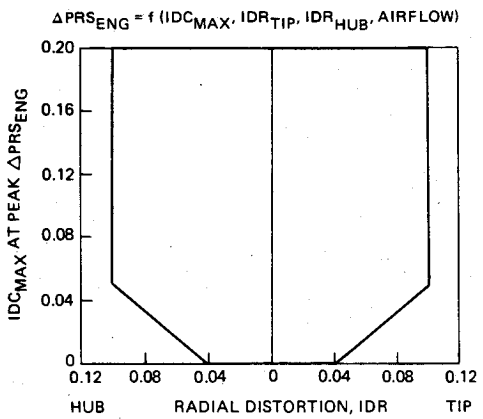

Fig. 6 Engine distortion experience boundary.

maintain satisfactory pressure lag and frequency response characteristics on the reference side. Analysis indicates that no pneumatic lag errors are introduced on the reference pressure side in the 0-0.25 Hz range of interest.

High-Frequency Response Pressure Measurement System

The high-response transducer system consists of 40 rake-mounted probe assemblies, located next to the low-response probes, which measure fluctuating pressures in the 0.25-1000 Hz frequency range (Fig. 3). Use of separate high-response probes permits easy probe replacement and positive contact for transducer excitation power and signal leads. The absolute-pressure high-response transducer is a strain-gage-type semiconductor designed as an integral part of a replaceable probe assembly requiring only electrical connectors to the rake. Each probe assembly is attached to the rake strut beneath the removable forward fairings.

Matched "Crossover" Filters

Matched low- and high-pass crossover filters are used to filter extreme low-frequency signals from the low- and high-response transducers prior to recording. These crossover filters have a first-order roll-off characteristic with a "crossover" frequency of 0.25 Hz. A separate filter set is provided for each of the 40 low- and high-response transducers. Two additional low-pass filters are used for the two reference transducers. The filters' effect on the combined pressure signal accuracy is small. A small amplitude error (less than 0.5%) occurs at the 0.25 Hz crossover frequency, but attenuates rapidly to zero on either side of this frequency.

Low-Response Data Acquisition

The low-response data acquisition system consists of an onboard sampling and digitizing unit which supplies data to the onboard tape recorder. A general-purpose low-response data recording system is used to sample and digitize the low-response rake data. The 40 differential pressure transducers are sampled with 8-bit words. The two reference pressure transducers are sampled with 16-bit words for increased resolution accuracy over their 2-32 psia span. The time division multiplex system (TDMS) provides a pulse code-modulated digital output which is recorded on one track of the 14 track intermediate band magnetic tape recorder operating at 15 in./s. The low-response data acquisition rate is 10 samples which is the base rate of the TDMS. Because the data are filtered through 0.25 Hz first-order filters prior to sampling, this rate is sufficient to accurately define the waveforms and levels of the low-response pressure data.

High-Response Data Acquisition

The high-response data acquisition system is a signal multiplexing system which provides data to the onboard tape recorded in FM-multiplex form. The F/A-18A frequency division multiplex system (FDMS) utilizes constant bandwidth (±2 kHz) FM multiplex recording conforming to IRIG (Inter-Range Instrumentation Group) standards. Channel center frequencies are 8 kHz apart, beginning at 16 kHz. This system is used to record data containing frequencies of 0.25-1000 Hz. Six channels of data can be recorded on each track.

Compatibility Assessment Procedure

In assessing the impact of inlet distortion on a turbofan engine, the peak time variant distortion levels generated by the inlet at the inlet/engine interface and the engine sensitivity to these distortion levels must be evaluated. The distortion descriptors and the data editing procedures used to evaluate compatibility are presented in this section.

Compatibility Assessment Descriptors

The key inlet distortion parameters established by General Electric for the F404 engine are defined in terms of circumferential and radial indices as follows.

Circumferential Distortion

The maximum circumferential ring pressure distortion index (IDC_{MAX}) is determined by first calculating the index for each of the five rings and includes a circumferential extent factor as a multiplier on each ring. This factor is a function of the circumferential extent of the low-pressure region for each ring $(\theta^{-})_{ring_i}$ and is empirically derived from engine and component test data,

$$IDC_{ring_i} = \frac{[P_{AV_{ring_i}} - P_{MIN_{ring_i}}]F(\theta^{-})_{ring_i}}{P_{AV_{FACE}}}$$

where each of the parameters is defined as

$P_{AV_{ring_i}}$ = area- averaged total pressure of ring *i*, psia
$P_{MIN_{ring_i}}$ = minimum total pressure of ring *i*, psia
$P_{AV_{FACE}}$ = area-averaged total pressure over the complete face, psia
$F(\theta^{-})_{ring_i}$ = circumferential extent factor

and IDC_{MAX} is largest of one of the following:

$IDC_{HUB} = \frac{1}{2}(IDC_{ring\,1} + IDC_{ring\,2})$
$IDC_{MIDH} = \frac{1}{2}(IDC_{ring\,2} + IDC_{ring\,3})$
$IDC_{MIDT} = \frac{1}{2}(IDC_{ring\,3} + IDC_{ring\,4})$
$IDC_{TIP} = \frac{1}{2}(IDC_{ring\,4} + IDC_{ring\,5})$

Radial Distortion

The radial distortion indices are defined using the IDR term and include both hub or tip radial distortions,

$$IDR_{ring_i} = \frac{P_{AV_{FACE}} - P_{AV_{ring_i}}}{P_{AV_{FACE}}}$$

IDR_{MAX} is largest of $IDR_{ring\,5}$ or $IDR_{ring\,1}$. If IDR_{MAX} is located in ring 5, the distortion is tip radial (IDR_{TIP}). If

IDR_{MAX} is located in ring 1, the distortion is hub radial (IDR_{HUB}).

Engine Distortion Experience Boundary

Figure 6 shows the engine distortion experience boundary established during the F404 engine development by the engine manufacturer. It is based on extensive full-scale engine testing using distortion screens and other distortion generating devices (i.e., random frequency generator). Key inlet dynamic distortion parameters (IDC_{MAX}, IDR_{TIP} and IDR_{HUB}) were monitored during postflight compatibility analysis at peak levels of the engine distortion sensitivity parameter (ΔPRS_{ENG}).

Analog Distortion Calculator

A special-purpose, hard-wired, analog distortion calculator (ADC) was designed and built for F/A-18A inlet distortion data computations and editing. The low- and high-response data which are recorded on the airborne data tape are played back through the ADC for editing. The ADC computes values of the distortion parameters by combining, in real time, the 40 high-response pressure signals, the 40 low-response differential pressure signals, and the reference pressure signal. Prior to entering the ADC computation section, the high-response data are filtered using 40 four-pole, linear-phase, low-pass filters with a 3 dB down point of 105 Hz. These filters are required to obtain data within the frequency range to which the engine is sensitive.

All of the dynamic distortion parameters required for the compatibility assessment are calculated by the ADC and recorded on both strip charts and tape in analog waveforms. For each of these calculated parameters, the ADC provides a parameter time history, a peak value that updates with each successively higher peak, and a worst-case flagging signal which is output each time successively higher peaks are calculated. In addition, it has built-in sample-and-hold capability: each time peak ΔPRS_{ENG} updates, the corresponding values (or "snapshots") of the three key distortion components (IDC_{MAX}, IDR_{TIP} and IDR_{HUB}) are output along with peak ΔPRS_{ENG}.

During the compatibility flight test program, inlet dynamic distortion data were calculated and edited during postflight processing of the flight data tape through the ADC. The analog calculated distortion data were then screened to select the distortion points at peak engine sensitivity (ΔPRS_{ENG}) for digitization. Digital processing was limited to points where the analog distortion levels were high or where dynamic distortion patterns were desired. One-half second segments of dynamic data were selectively digitized around peak ΔPRS_{ENG}. Digitized distortion output included waveforms and distortion contour plots calculated from the digitized probe data. Figure 7 shows a waveform comparison of analog and digitized data indicating good comparison in both level and waveform integrity.

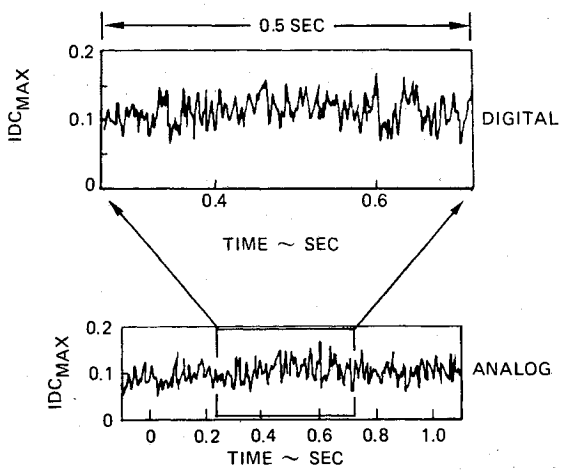

Fig. 7 Analog-to-digital waveform comparison.

Compatibility Flight Test Results

The overall scope of the inlet/engine compatibility flight test program conducted on the instrumented propulsion test aircraft (F2), is shown in Fig. 8. A total of 24 compatibility flights were flown on F2 with about 360 distortion data points digitized during the flight test program. All of the critical maneuvering conditions, both subsonic and supersonic, were flight tested with special emphasis on the F/A-18A prime combat maneuvering region. The objective was to demonstrate a compatible inlet/engine system within the design goal maneuvering envelopes for both fixed and variable throttle.

Inlet Distortion

In the discussions that follow, inlet distortion patterns are included where necessary to show the range of dynamic distortion activity at the engine face during extreme aircraft maneuvering attitudes. When discussing engine sensitivity to inlet distortion, it is important to note that engine components are sensitive to pressure distortion patterns, but not to the distortion parameters. The latter are just tools used to identify as accurately as possible the time at which the worst instantaneous pressure distortion pattern occurs during any given aircraft maneuver. During the digitization process, instantaneous (i.e., peak time variant) pressure distortion patterns were generated at the worst (i.e., at peak engine sensitivity) time slice within the 0.5 s digitized data segment. The low-frequency response data were used to generate the corresponding steady-state distortion contour at the same time.

Angle of Attack Effects on Distortion

Flight test inlet distortion data trends with angle of attack at zero sideslip show an increase in inlet distortion with angle of attack (Fig. 9a). Both circumferential and radial distortion results are presented. The data show rapid increase in circumferential inlet distortion with angle of attack. This increase is related to inlet lip flow separation effects as angle of attack is increased. Four dynamic distortion patterns at the engine face at increasing angles of attack are shown in Fig. 9b to graphically illustrate this increase in distortion. The patterns show contour lines in 2% increments above and below the heavy average pressure line. The increase in dynamic distortion pattern intensity (differential pressure across pattern) can be clearly seen with increasing angle of attack.

Sideslip Effects on Distortion

The rapid increase in inlet dynamic distortion with leeward sideslip is shown in Fig. 10 at two representative angles of attack. The substantial increase in distortion when the aircraft attitude changes from windward to leeward sideslip can be

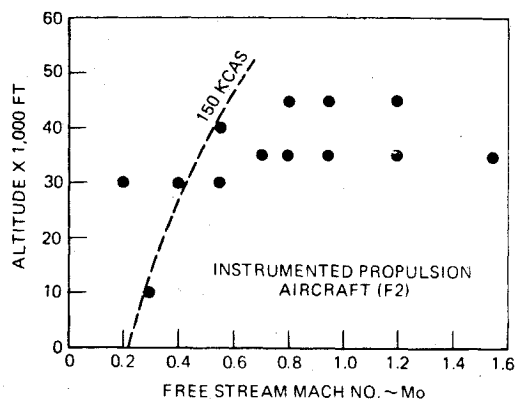

Fig. 8 Compatibility flight test points.

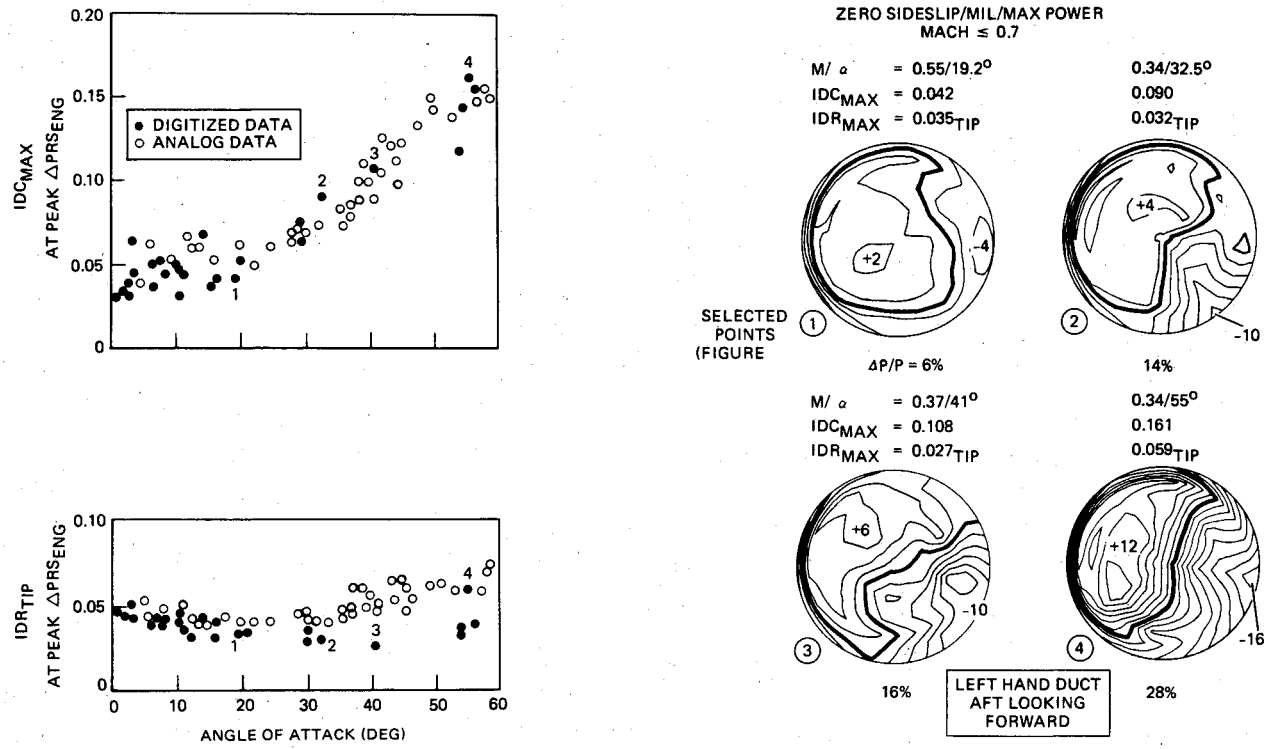

Fig. 9 Angle-of-attack effect on dynamic inlet distortion.

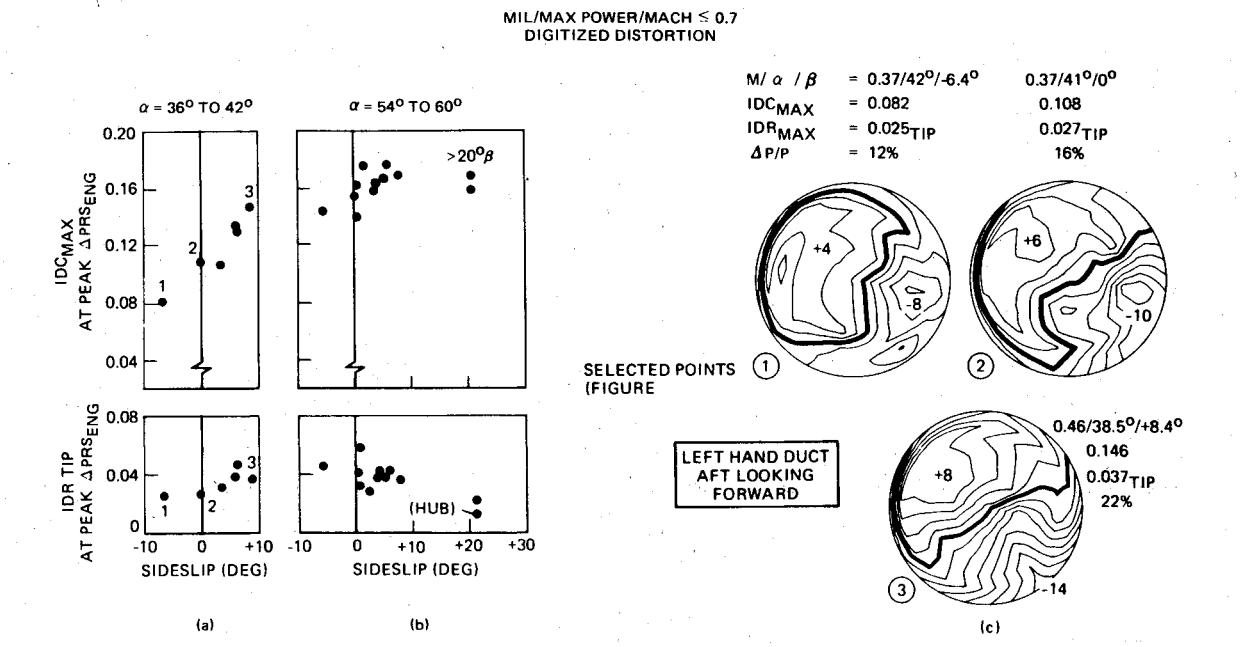

Fig. 10 Angle-of-sideslip effect on dynamic inlet distortion.

clearly seen in Fig. 10a. Three dynamic distortion patterns illustrate this graphically in Fig. 10c. Figure 10b shows the same effect with sideslip at a considerably higher angle of attack.

Inlet/Engine Compatibility

In order to demonstrate a compatible inlet/engine system, measured dynamic inlet distortion levels obtained during extreme F2 maneuvers are compared with the engine distortion experience boundary established during the F404 engine development by the engine manufacturer. Subsonic compatibility assessments are discussed for both fixed and variable throttles. Supersonic fixed-throttle compatibility is also presented.

Subsonic Compatibility (Fixed Throttle)

The overall fixed-throttle subsonic maneuvering envelope achieved by the instrumented aircraft is shown in Fig. 11a. Extreme excursions experienced by the aircraft during the flight test program with no engine stalls are used to define this boundary. Superimposed on the same figure is the fixed-throttle design goal envelope used during the development phase of the F/A-18A program in order to emphasize the extent to which the achieved envelope exceeds it. The aircraft fixed-throttle maneuvering attitudes at key digitized peak distortion points are also presented in Fig. 11b to show the scope of the distortion data base used in the discussion that follows. The range of measured data extends well outside the

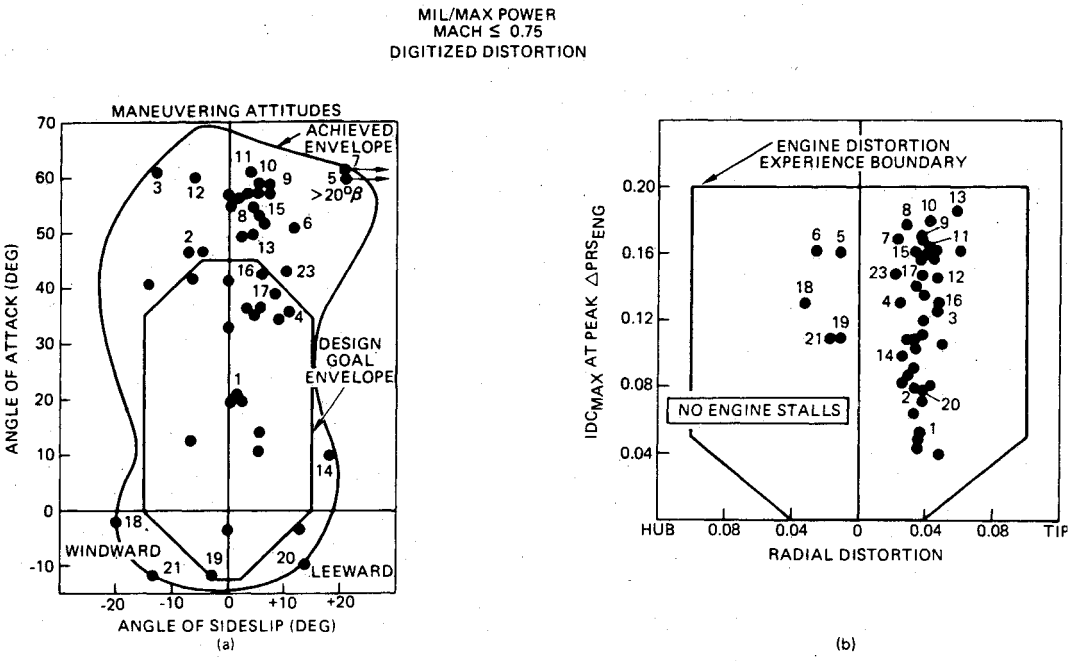

Fig. 11 Subsonic fixed throttle compatibility.

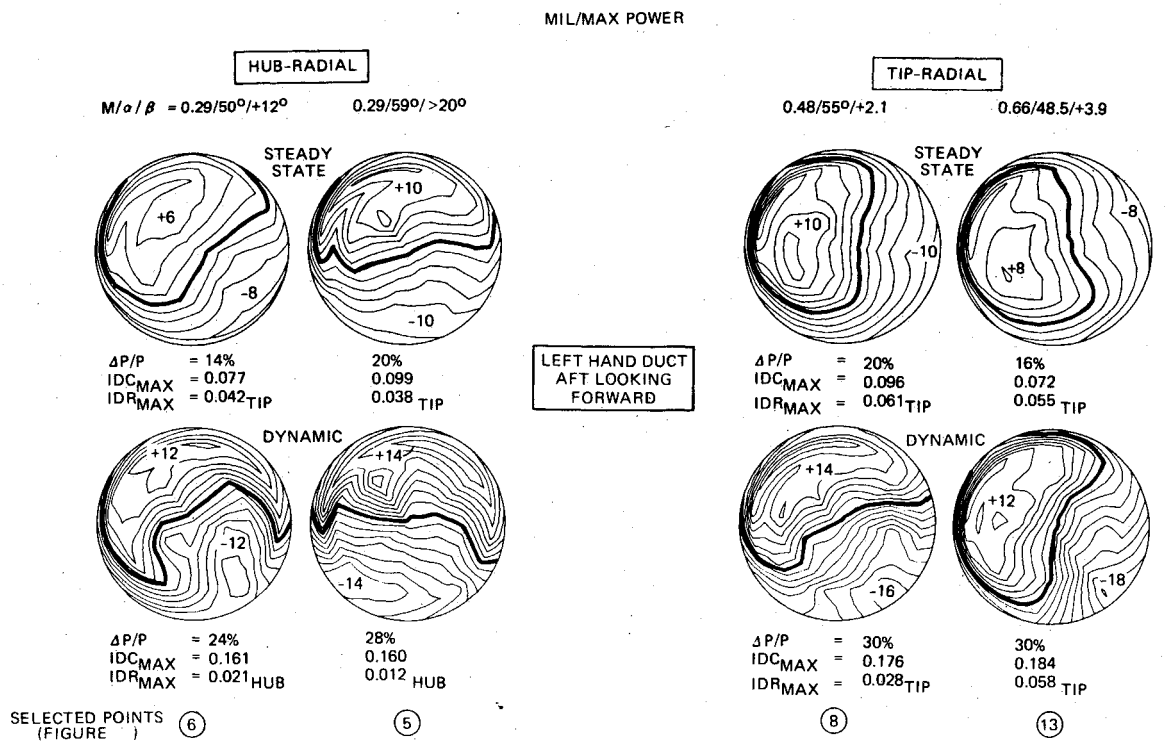

Fig. 12 High inlet distortion patterns.

design goal envelope. Extreme negative g maeuvering attitudes are also included.

Selected test points are sequentially numbered on the angle-of-attack/sideslip plot in order to key them to inlet distortion levels identified on the engine distortion experience boundary (Fig. 11b). No engine stalls occurred during the instrumented aircraft compatibility testing and all the points fall within the engine experience boundary. The measured distortion points have provided a comprehensive quantitative data base in terms of the angles of attack and sideslips achieved (Fig. 11a). The data show that the F/A-18A inlet generates predominately tip-radial distortion. Distortion levels for extreme negative g maneuvers (points 18-20) are lower and also within the engine distortion experience boundary. The quantitative distortion data obtained on F2 show that the inlet/engine system is compatible for subsonic maneuvering excursions well beyond the fixed-throttle design goal envelope.

Figure 12 shows peak time variant and the corresponding steady-state patterns for the two highest hub-radial and the two highest tip-radial distortion points (5, 6 and 8, 13, respectively). These points represent some of the highest

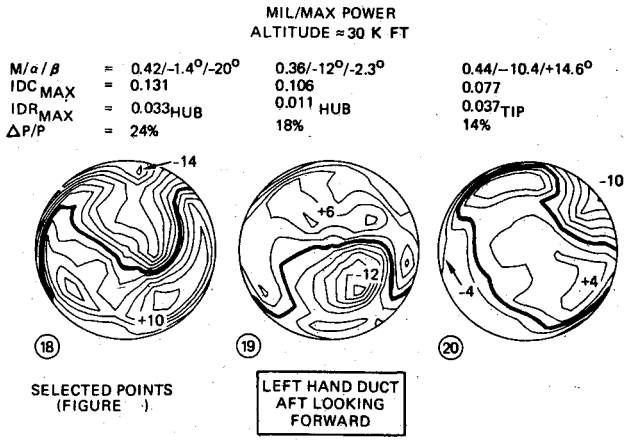

Fig. 13 Negative *g* maneuvering dynamic distortion patterns.

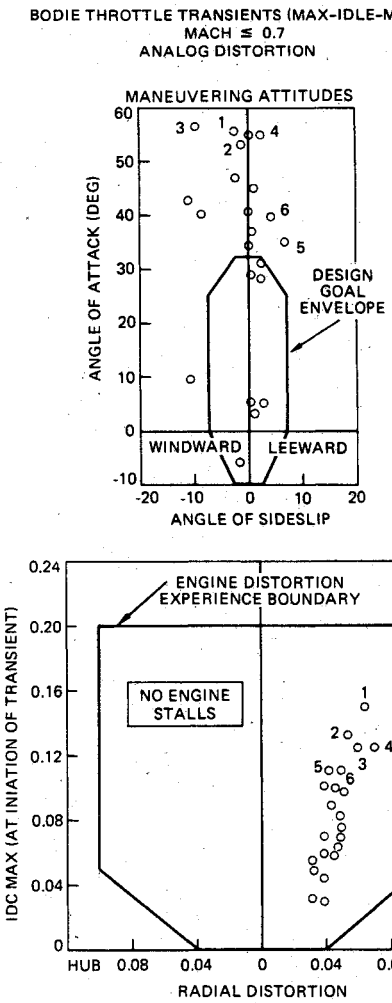

Fig. 14 Subsonic variable throttle compatibility.

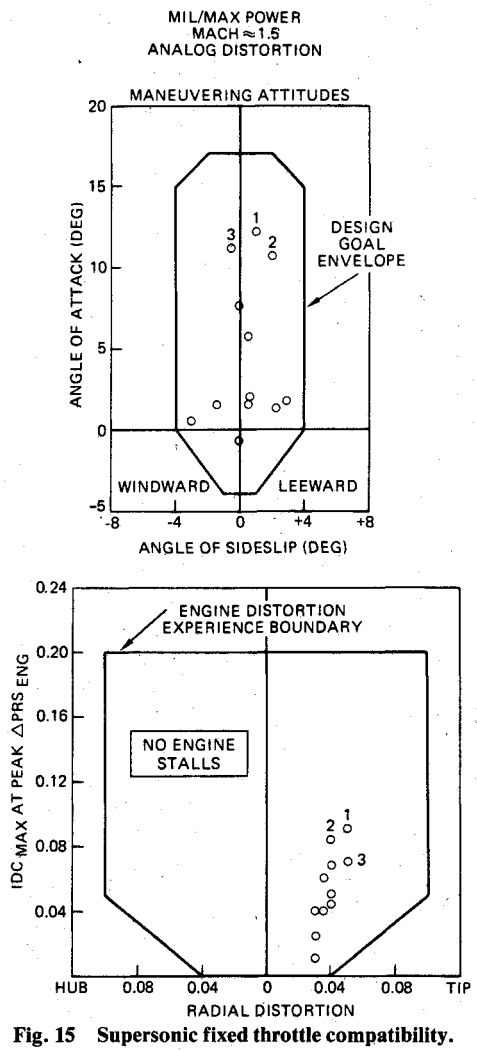

Fig. 15 Supersonic fixed throttle compatibility.

measured levels of flight distortion. The dynamic patterns are much more intense than the steady-state patterns, as indicated by the corresponding pattern differential pressure levels.

Figure 13 shows dynamic distortion patterns for negative *g* maneuvering points (18-20) at three extreme flight attitudes. The patterns show the change in distortion from hub-radial to tip-radial as the aircraft attitude changes from windward to leeward sideslip. The location of the low-pressure zone is also shifted with respect to the high distortion points (5, 6, 8, and 13) due to the negative aircraft angle of attack.

Subsonic Compatibility (Variable Throttle)

The procedure adopted to demonstrate inlet/engine compatibility for variable throttle during the flight test program was to fly fixed throttle to a desired target flight condition and attitude and initiate an engine "bodie" (max-idle-max) throttle movement. A bodie was considered to be the most critical transient with respect to engine stall margin loss.

The aircraft maneuvering attitudes at which the key engine bodies were performed are shown in Fig. 14a. The variable-throttle design goal envelope is superimposed and shows that the engine transients were performed well beyond this envelope.

Figure 14b shows the selected test points sequentially numbered on Fig. 14a in order to key them to the inlet distortion levels at the time the transient was initiated. All of the data points fall well within the engine distortion experience boundary. Again, no engine stalls occurred during the instrumented aircraft variable throttle compatibility testing, demonstrating that the inlet/engine system is compatible for variable throttle to attitudes well beyond the design goal envelopes.

Supersonic Compatibility

Representative supersonic maneuvering flight test points shown in Fig. 15 quantify the F/A-18A inlet distortion levels experienced during fixed-throttle supersonic maneuvers. The F/A-18A aerodynamic characteristics are such that the supersonic maneuvering attitudes are significantly lower than

the corresponding subsonic maneuvering attitudes. Supersonic maneuvering distortion levels experienced by the inlet are low and well within the engine distortion experience boundary. Supersonic variable-throttle compatibility is the same as fixed-throttle compatibility since the F404 engine incorporates a control feature which limits airflow to mil/max power levels during throttle transients at supersonic flight conditions. No engine stalls occurred during the supersonic compatibility evaluation.

Conclusions

The F/A-18A flight test program has explored the inlet/engine system compatibility in detail with excellent results. All of the design goals have been achieved based on the following conclusions:

1) The inlet instrumentation and data acquisition system operated satisfactorily throughout the compatibility flight test program.

2) No engine stalls occurred during the fixed- or variable-throttle compatibility testing for subsonic maneuvering excursions well beyond the design goal envelopes. The distortion points fall within the engine distortion experience boundary. Satisfactory engine operation has been demonstrated, and inlet distortion measured up to 65 deg angle of attack and 20 deg sideslip.

3) Compatible subsonic maneuvering excursions well beyond the variable-throttle design goal envelopes are also demonstrated on the instrumented aircraft using the worst-case throttle transient (max-idle-max bodie).

4) Inlet dynamic distortion levels during supersonic aircraft maneuvers are low and well within the engine distortion experience boundary.

References

[1]Farr, A. P., "Evaluation of F-15 Inlet Dynamic Distortion," AIAA Paper 73-784, Aug. 1973.

[2]Farr, A. P. and Schumacher, G.A., "System for Evaluation of F-15 Inlet Dynamic Distortion," *AIAA Progress in Astronautics and Aeronautics Instrumentation for Airbreathing Propulsion,* Vol. 34, edited by A.E. Fuhs and M. Kingery, AIAA, New York, 1974, pp. 59-76.